Journal of Trace Elements in Medicine and Biology xxx (xxxx) xxx–xxx

Contents lists available at ScienceDirect

Journal of Trace Elements in Medicine and Biology

journal homepage: www.elsevier.com/locate/jtemb

Analytical methodology

Characterization of Caco-2 cells stably expressing the protein-based zinc probe eCalwy-5 as a model system for investigating intestinal zinc transport

Maria Maares[a], Claudia Keil[a], Susanne Thomsen[a], Dorothee Günzel[b], Burkhard Wiesner[c], Hajo Haase[a,d,*]

[a] Department of Food Chemistry and Toxicology, Berlin Institute of Technology, Berlin, Germany
[b] Institute of Clinical Physiology, Charité - Universitätsmedizin Berlin, Campus Benjamin Franklin, Berlin, Germany
[c] Leibniz Institute for Molecular Pharmacology, Berlin, Germany
[d] TraceAge—DFG Research Unit on Interactions of essential trace elements in healthy and diseased elderly, Potsdam-Berlin-Jena, Germany

ARTICLE INFO

Keywords:
Zinc
Intestinal cell model
Caco-2
Zinc-biosensor
eCalwy

ABSTRACT

Intestinal zinc resorption, in particular its regulation and mechanisms, are not yet fully understood. Suitable intestinal cell models are needed to investigate zinc uptake kinetics and the role of labile zinc in enterocytes *in vitro*. Therefore, a Caco-2 cell clone was produced, stably expressing the genetically encoded zinc biosensor eCalwy-5. The aim of the present study was to reassure the presence of characteristic enterocyte-specific properties in the Caco-2-eCalwy clone. Comparison of Caco-2-WT and Caco-2-eCalwy cells revealed only slight differences regarding subcellular localization of the tight junction protein occludin and alkaline phosphatase activity, which did not affect basic integrity of the intestinal barrier or the characteristic brush border membrane morphology. Furthermore, introduction of the additional zinc-binding protein in Caco-2 cells did not alter mRNA expression of the major intestinal zinc transporters (*zip4*, *zip5*, *znt-1* and *znt-5*), but increased *metallothionein 1a*-expression and cellular resistance to higher zinc concentrations. Moreover, this study examines the effect of sensor expression level on its saturation with zinc. Fluorescence cell imaging indicated considerable intercellular heterogeneity in biosensor-expression. However, FRET-measurements confirmed that these differences in expression levels have no effect on fractional zinc-saturation of the probe.

1. Introduction

The essential trace element zinc plays an important role for a variety of biological processes in the human body [1]. Zinc homoeostasis is mainly dependent on dietary intake and bioaccessibility from food in the intestine, where zinc is resorbed [2]. Intestinal zinc homeostasis is primarily mediated by four zinc transporters: zinc uptake from the gastrointestinal lumen is controlled by ZIP4, which is expressed on the apical membrane of the intestinal epithelium, whereas ZIP5 at the basolateral membrane transports zinc from the blood into enterocytes. The zinc exporters ZnT-1 and ZnT-5 are essential for zinc transport from the enterocytes into the blood or back into the intestinal lumen, respectively [3]. Despite ongoing research [4], knowledge of the amount of labile zinc and zinc uptake kinetics in intestinal cells is scarce. In particular, the mechanism and regulation of human zinc resorption is not fully understood [5].

There are several ways to investigate cellular zinc resorption *in vitro*. Alongside the quantification of whole cellular zinc using analytical methods such as ICP-MS (inductively-coupled plasma mass spectrometry) and FAAS (flame atomic absorption spectrometry) [6], fluorescence-based sensors are increasingly used to study intracellular free zinc [7,8]. Recently, several genetically encoded fluorescent sensor proteins have been developed to analyze intracellular labile zinc. Among them are the eCalwy sensors from the Merkx group, which are based on Förster Resonance Energy Transfer (FRET) between two fluorescent domains bound to the metal binding domains WD4 and ATOX1, connected by a flexible linker [9]. Upon zinc binding, FRET is decreasing because of conformational change and growing distance

Abbreviations: ANOVA, analysis of variance; ALP, alkaline phosphatase; Calwy, CFP-Atox1-linker-WD4-YFP; DAPI, 4′,6-diamidin-2-phenylindole; DMEM, Dulbecco's Modified Eagle's Medium; FAAS, flame atomic absorption spectrometry; FCS, fetal calf serum; FLIM, fluorescence lifetime imaging microscopy; FRET, Förster resonance energy transfer; ICP-MS, inductively-coupled plasma mass spectrometry; LC, lethal concentration; MTT, 3-(4,5-dimethylthiazol-2-yl)-2,5-diphenyltetrazolium bromide; pNPP, p-nitrophenyl phosphate; SEM, scanning electron microscopy; SRB, sulforhodamine B; TEM, transmission electron microscopy; TPEN, N,N,N′,N′-Tetrakis(2-pyridylmethyl)ethylenediamine; WST, water soluble tetrazolium; ZnT, zinc transporter; ZIP, Zr,Irt-like transporter

* Corresponding author at: Department of Food Chemistry and Toxicology, Berlin Institute of Technology, Gustav-Meyer-Allee 25, D-13355 Berlin, Germany.
E-mail address: Haase@TU-Berlin.de (H. Haase).

https://doi.org/10.1016/j.jtemb.2018.01.004
Received 6 November 2017; Received in revised form 22 December 2017; Accepted 17 January 2018

between the donor-domain (cerulean) and the acceptor mCitrine. Zinc-biosensors offer several advances compared to synthetic sensors. They are produced by the cell itself, providing control over their subcellular distribution and concentration and are well-suited for long term-measurements [10,11]. In this sense, applying these sensors in enterocytes would be suitable to monitor free zinc in these cells and illuminate sensitive parameters of intestinal zinc resorption. Therefore, a Caco-2 cell clone was produced stably expressing eCalwy-5.

Future research aims to include Caco-2-eCalwy-5 cells in *in vitro* models for the intestinal epithelium. Therefore, this study investigates if characteristic properties of the wildtype cells are conserved in the stably transfected cell clone and examines the effect of sensor-expression level on its zinc-saturation.

2. Experimental

2.1. Materials

ApaLI (NEB, Ipswich, USA), Cell Counting Kit-8/WST-8 (Sigma Aldrich, Munich, Germany), Cy-2-labeled goat anti mouse and Cy-5-labeled goat anti rabbit secondary antibodies (Jackson ImmunoResearch, Dianova, Hamburg, Germany), Claudin 2 polyclonal antibody, Occludin monoclonal antibody and ZO-1 polyclonal antibody (Invitrogen, ThermoFisher Scientific, USA), Cloning cylinders (Sigma Aldrich, Munich, Germany), DAPI (Invitrogen, ThermoFisher Scientific, USA), DMEM (PAN-Biotech, Aidenbach, Germany), FCS (CCPro, Oberdorla, Germany), G 418 disulfate (Geneticin) (Santa Cruz Biotechnology, Dallas, Germany), Invisorb Spin Tissue Mini Kit (Stratec Molecular GmbH, Berlin, Germany), iScript cDNA Synthesis Kit (Quantabio, Beverly, USA), Lipofectamin 2000 (Invitrogen, ThermoFisher Scientific, USA), MTT (Carl Roth, Karlsruhe, Germany), NucleoSpin II (Macherey-Nagel GmbH & Co. KG, Berlin, Germany), Opti-Mem (Sigma Aldrich, Munich, Germany), PCR Clean-Up System (Promega, Madison, USA), peCalwy-plasmid (addgene, Cambridge, USA), pNPP (PanReac AppliChem, Glenview, USA), PNP (Sigma Aldrich, Munich, Germany), ProTaqs Mount Fluor (Biocyc, Luckenwalde, Germany), Purified Mouse Anti-E-Cadherin (BD Transduction Laboratories™, BD Biosience, New Jersey, USA), SYBR™-Green (Quantabio, Beverly, USA), Transwell inserts (Corning, New York, USA), TPEN (Sigma Aldrich, Munich, Germany), Qiagen Plasmid Maxi Kit (Qiagen, Venlo, Netherlands), $ZnSO_4 \times 7H_2O$ (Sigma Aldrich, Munich, Germany). All other chemicals were purchased from standard sources.

2.2. Cell culture

Cells were cultured at 37 °C, 5% CO_2 and humidified atmosphere in Dulbecco's Modified Eagles Medium (DMEM), containing 10% fetal calf serum (FCS), 100 U/mL penicillin and 100 g/ml streptomycin. Media were changed every other day. A final concentration of 0.6 mg/mL G418 was added to Caco-2-eCalwy clones.

2.3. Stable transfection

Plasmid-DNA of peCalwy-5 was introduced to *E. coli*, isolated using Qiagen Plasmid Maxi Kit and purified using Invisorb Spin Tissue Mini Kit, according to the manufacturers' protocols. Purified peCalwy-5-DNA was linearized using ApaLI and successful linearization was confirmed by gel-electrophoresis. Finally, $4*10^4$ Caco-2-WT cells were seeded into 24 well-plates, cultivated for 24 h and transfected by adding a total of 0.5 µg plasmid DNA and 2.5 µg Lipofectamin 2000 directly to the medium. After additional 24 h, medium was changed and transfection was checked by fluorescence microscopy. 48 h after transfection 1.2 mg/mL G 418 disulfate was added to cells and cultured for additional 6 days. Finally cells were transferred to a 100 cm^2 dish and isolated cell clones were selected, picked by using cloning cylinders and transferred into 24 well plates.

2.4. Alkaline phosphatase activity

Alkaline phosphatase (ALP) catalyzes the hydrolyzation of pNPP to yellow *p*-nitrophenol, which can be measured photometrically at 405 nm. Extracellular ALP-activity was analyzed on live cultured cells according to the method described by Ferruzza et al. [12]. Caco-2 clones (5000 cells/well) were cultured for 21 days in 96 well plates, washed with PBS, and 10 mM pNPP in reaction buffer (10 mM Tris-HCl, 150 mM NaCl, pH 8.0) was added to the cells. Samples were collected at different time points and *p*-nitrophenol was quantified using an external calibration. Protein was quantified using the BCA-assay as described [13] and ALP-activity is depicted in mU/mg protein (Hydrolyzation of 0.346 nmol pNPP/min = 1 mU ALP).

2.5. Immunofluorescent staining

Immunofluorescence analysis was performed with cells ($8*10^4$ cells/well) grown on polycarbonate transwell membranes (pore size 0.4 µm) for 21d. Cell culture media were changed every other day and integrity of the cell layer was monitored by measuring TEER (transepithelial electrical resistance) with the epithelial volt-ohm meter Millicell® ERS-2 (Millipore, USA). Differentiated cells were washed with PBS, fixed with 2% paraformaldehyde for 20 min at room temperature and permeabilized with 0.5% Triton-X-100 in PBS for 10 min. Cells were incubated overnight at 4 °C with primary antibodies against claudin-2, occludin, *zonula occludens*-1 (ZO-1) protein and E-cadherin diluted 1:200 in PBS. After three washes, cells were incubated with Cy-2-labeled goat anti mouse and Cy-5-labeled goat anti rabbit secondary antibodies and 4′,6-diamidino-2-phenylindole (DAPI) (final concentration 1 µg/mL) for 45 min at room temperature. Subsequently cells were washed, dehydrated with 95% ethanol and mounted in ProTaqs Mount Fluor. The mounting medium was allowed to solidify for 1 h in the dark, before fluorescence measurements were performed using confocal laser scanning microscopy (Zeiss LSM780) at excitation wavelengths of 488 nm (Cy-2), 633 nm (Cy-5) and 405 nm (DAPI).

2.6. Transmission electron microscopy (TEM) and scanning electron microscopy (SEM)

Cells grown on cover slips ($6*10^4$ cells/well; 12 well plates), were fixed with 2.5% glutaraldehyde in 0.1 M sodium-cacodylat buffer for 30 min at room temperature and dehydrated trough a graded series of ethanol. TEM imaging was performed using an EM906 (Zeiss, Germany). SEM measurements were conducted with a DSM982Gemini (Zeiss, Germany).

2.7. Viability assays

Cells were seeded with an initial density of 5000 cells/well in 96 well plates and cultured for 21d. For acute zinc toxicity, differentiated cells were incubated with 0–1000 µM $ZnSO_4 \times 7H_2O$ for 24 h in DMEM without phenol red and fetal calf serum. Subsequently, cells were washed with PBS and cell viability was analyzed incubating either with the water soluble tetrazolium salt (WST)-8 (diluted 1:10) or 1 mg/mL 3-(4,5-Dimethylthiazol-2-yl)-2,5-diphenyltetrazolium bromide (MTT) in DMEM without phenol red for 30–60 min. In case of the MTT-assay cells were lysed in isopropanol. The absorption was determined on a well plate reader (M200, Tecan, Swiss) at 490 nm (WST) or 570 nm (MTT), respectively. A total of 0.01% Triton-X-100 was used as a positive control. Data were analyzed with GraphPad Prism software version 5.01 (GraphPad Software Inc., CA, USA) and a non-linear regression using a sigmoidal dose–response curve with variable slope as a function of the logarithm of concentration was applied. Chronic zinc toxicity was measured by incubating the cells with 0, 5 and 10 µM $ZnSO_4 \times 7H_2O$ in

Table 1
Oligonucleotide sequences used for real-time PCR.

Primer	NCBI Reference Sequence	Sequence fwd 5′-3′	Sequence rev 5′-3′	Ref
ZIP-4	NM_017767	AGACTGAGCCCAGAGTTGAGGCTA	TGTCGCAGAGTGCTACGTAGAGGA	[15]
ZIP-5	NM_173596	GAGCAGGAGCAGAACCATTACCTG	CAATGAGTGGTCCAGCAACAGAAG	[15]
ZnT1	NM_021194	GGCCAATACCAGCAACTCCAA	TGCAGAAAAACTCCACGCATGT	[16]
ZnT5	NM_024055	AAGGACATCATGACAGTGCTCTAACTC	CCAACTTTACAACACAAAGCCAGTAC	[16]
MT1a	NM_005946.2	CTCCTGCAAGAAGAGCTGCTG	CAGCCCTGGGCACACTT	
ALP	NM_001631.4	CCGCTTTAACCAGTGCAACA	CCCATGAGATGGGTCACAGA	
β-actin	NG_007992.1	CGCCCCAGGCACCAGGGC	GCTGGGGTGTTGAAGGT	[17]

standard cell culture medium during differentiation. Cell viability of differentiated cells was measured as the amount of cellular protein using the sulforhodamine B (SRB)-assay as described [14].

2.8. Quantitative real time PCR (qPCR)

$1.2*10^5$ cells were seeded in 6 well plates and cultured for 21d. Cells were harvested in PBS on ice using a cell scraper, and cell pellets were stored at −80 °C. RNA was isolated with Nucleo Spin II and cDNA synthesized using iScript cDNA Synthesis Kit according to the manufacturers' protocols. Finally, mRNA-levels were quantified by qPCR with SYBR™Green Super Mix, using the primer listed in Table 1, and normalized to β-actin.

2.9. Atomic absorption spectrometry

$1.2*10^5$ cells were seeded in 6 well plates and cultured for 21d. Cell layers were harvested on ice with a cell scraper, and an aliquot was collected for protein quantification as described [13]. Subsequently cells were dissolved in a mixture of 67% ultrapure HNO_3 and 30% H_2O_2 (50/50; v/v) and dried at 92 °C overnight using a thermoshaker. Residues were dissolved in 0.67% HNO_3 and samples were analyzed by FAAS using a Perkin Elmer AAnalyst800 (Perkin Elmer, Germany).

2.10. Live cell imaging and FRET-measurements

Confluent Caco-2-eCalwy cells on cover slips were used for live cell imaging with a confocal laser scanning microscope (Zeiss LSM710, Germany). Cells were washed twice with buffer (120 mM NaCl, 5.4 mM KCl; 5 mM Glucose; 1 mM $CaCl_2$; 1 mM $MgCl_2$; 1 mM NaH_2PO_4; 10 mM HEPES; pH 7.35) and a fluorescence emission scan was conducted after excitation at 458 nm (40×/1.3 oil objective; λ_{em} = 462nm–590 nm). Additionally, an emission scan of the acceptor-domain mCitrine was measured after direct excitation at λ_{ex} = 514 nm (λ_{em} = 526nm–590 nm). FRET is expressed as the fluorescence intensity ratio of mCitrine (λ_{em} = 527 nm) and cerulean (λ_{em} = 478 nm) after excitation at 458 nm. Ratios were measured in buffer alone (R_{apo}), or 10 min after the addition of 20 µM TPEN (R_{max}) or 400 µM zinc (R_{min}) (final concentrations). The measurements using a multiphoton laser scanning microscope (Zeiss LSM510-META-NLO, Germany) were conducted as described above, but after multiphoton excitation (810 nm) using a tunable IR-laser (λ_{em}(cerulean) = 478 nm, λ_{em}(mCitrine) = 532 nm).

The concentration of free zinc was determined using the following equation [11,18] and a dissociation constant for the zinc-eCalwy-5-complex of 1.85 nM [9]: $[Zinc] = Kd*[(R_{apo} - R_{max})/(R_{min} - R_{apo})*(S_{f2}/S_{b2})]$. The proportionality coefficients S_{f2} and S_{b2} are corresponding to the emission intensities of the free and bound forms of the sensor at 532 nm.

2.11. Fluorescence lifetime imaging microscopy (FLIM)-FRET

FLIM-measurements were performed with Caco-2-eCalwy cells using a multiphoton LSM510-META microscope equipped with a time-resolved LSM upgrade setup (Becker&Hickl, Germany). FLIM of the donor-domain cerulean was measured in buffer and in the presence of 20 µM TPEN or 400 µM zinc (40×/1.3 oil objective, λ_{ex} = 810 nm, 450–490 nm band pass filter). To analyze FLIM of cerulean in the absence of the acceptor domain mCitrine, Caco-2-WT clones were transfected with a cerulean-construct. FLIM data were analyzed using the SPC Image software from Becker&Hickl and FRET-efficiency was calculated using the following equation: $E(\%) = (1 - (\tau_{DA}/\tau_D))*100$, where τ_{DA} is the fluorescence lifetime of the donor-domain cerulean in intact eCalwy-protein and τ_D in the absence of mCitrine.

2.12. Statistical analysis

Statistical significance was analyzed by Student's *t*-test (for paired samples), or one- or two-way analysis of variance (ANOVA) (for multiple comparisons), followed by Bonferroni or Dunnetť's multiple comparison post hoc tests, as indicated in the respective figure legends, using GraphPad Prism software version 5.01 (GraphPad Software Inc., CA, USA). Error bars represent standard deviation of three independent biological replicates.

3. Results

3.1. Characteristic cellular features

To ensure the presence of characteristic features of the intestinal cell line Caco-2 after introduction of eCalwy-plasmids, cell differentiation, morphology, as well as barrier integrity were investigated. First, activity and expression of the differentiation marker alkaline phosphatase were compared. Both cells expressed large amounts of functional ALP; however, ALP-activity and -expression by Caco-2-eCalwy were significantly lower (each $p < 0.001$, Fig. 1) compared to wild type cells.

Ultrastructure comparison by TEM detected no remarkable differences in brush border formation. Fig. 2 shows the distribution of mitochondria, lysosomes, desmosomes, nexus and tight junctions, and microvilli of about 500–1000 nm length in differentiated cells. Notably, TEM images revealed the presence of more lysosomal structures in Caco-2-eCalwy. SEM images show the characteristic columnar shape of differentiated Caco-2-cells and evenly distributed microvilli on the surface of both cell clones (Fig. 3).

Barrier integrity, measured as TEER, did not differ between the two cell clones (Fig. SF1). Tight junction formation was analyzed using immunofluorescent staining of selected proteins: claudin-2, occludin, ZO-1 and E-cadherin (Figs. 4, SF2) to investigate whether stable transfection with eCalwy-5 had affected their distribution. Immunofluorescent images in Fig. 4 show the intracellular distribution of the tight junction proteins as x-y-scans and Fig. SF1 additionally depicts tight junction localization as z-scans together with stained nuclei. Localization and generation of claudin-2 and ZO-1 were not altered. Staining of claudin-2 revealed a membranous and cytoplasmic localization as well as a nuclear enrichment in Caco-2-WT and -eCalwy cells. In both cases, the peripheral protein ZO-1 displayed a homogenous localization in the cytoplasmic membrane. In contrast, immunofluorescent images of occludin and E-cadherin revealed slight

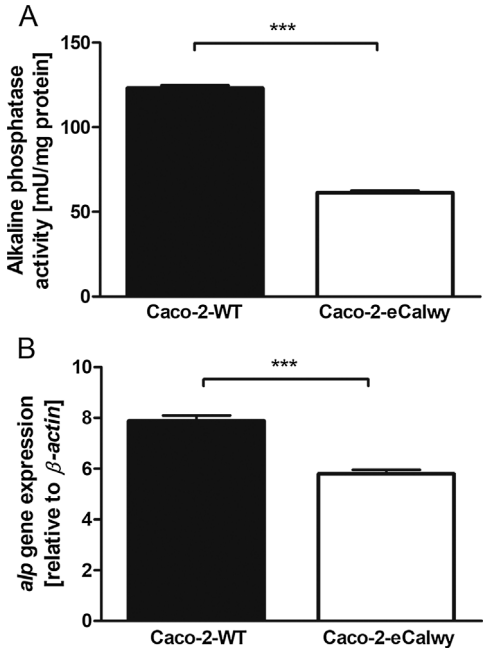

Fig. 1. Alkaline phosphatase (ALP) in Caco-2-WT and Caco-2-eCALWY cells. (A) Enzyme activity in differentiated cells was measured using an ALP-assay and is displayed relative to cellular protein. (B) Relative *alp* expression in differentiated cells was analyzed using qPCR. Data are shown as means ± SD of three independent experiments. Means of each cell clone are significantly different as indicated (***$p < 0.001$, Student's *t*-test).

differences. Occludin is located in the plasma membrane of Caco-2-WT, whereas it shows tendencies of a lateral staining, with decreasing sensitivity from apical to basolateral membrane, in Caco-2-eCalwy (Figs. 4B,F and SF2B,F). Imaging of E-cadherin revealed membranous distribution and vesicular accumulation of this protein in Caco-2-WT, whilst in eCalwy transfected cells E-cadherin was mostly found in the apical cell membrane with only a slight vesicular localization (Figs. 4D,H and SF2D,H).

3.2. Zinc homeostasis

The introduction of an additional zinc binding protein into Caco-2 cells might change zinc homeostasis in the stably transfected cell clone, potentially enhancing the resistance against elevated zinc concentrations, or increasing the requirement for zinc during growth and differentiation. Thus, viabilities of differentiated Caco-2-WT and -eCalwy after incubation with 0–1000 µM zinc for 24 h were compared by measuring mitochondrial activity (Fig. 5A,B). In contrast to Caco-2-WT, the Caco-2-eCalwy cells had higher LC_{50} values in MTT (865 µM *vs.* 394 µM for wildtype) and WST assays (803 µM *vs.* 427 µM for wildtype). Furthermore, cellular protein content after differentiation in the presence of different zinc concentrations was analyzed (Fig. 6). The amounts did not change in Caco-2-WT, whereas addition of 5 and 10 µM zinc to the culture media led to a slight but significant increase in Caco-2-eCalwy.

The expression of proteins important for zinc homeostasis in enterocytes, such as metallothionein 1a (*mt1a*) and the zinc transporters *zip4*, *zip5*, *znt-1* and *znt-5*, were examined (Fig. 7A). eCalwy-5 did not affect mRNA expression of zinc transporters, but significantly elevated *mt1a*-expression ($p < 0.05$) by 20%. In contrast, there were no significant differences in basal cellular zinc levels between Caco-2-WT and -eCalwy cells (Fig. 7B).

3.3. Functionality and application

Cellular distribution of the sensor-protein in Caco-2-eCalwy cells

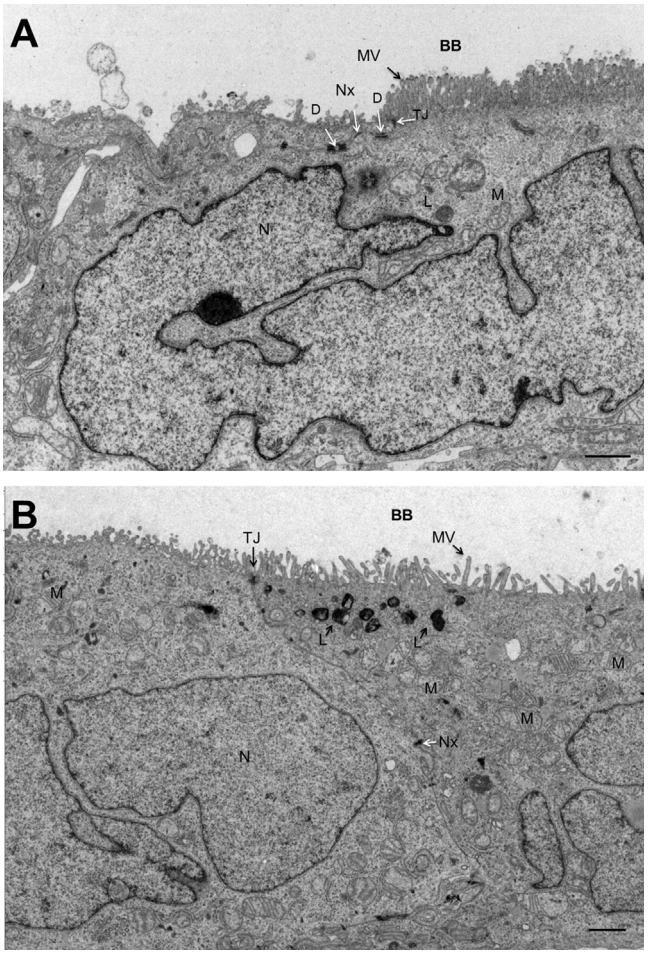

Fig. 2. Transmission electron micrographs. Differentiated Caco-2-WT clones (A) and Caco-2-eCalwy (B) were analyzed for typical features of the brush border (BB) of intestinal cells, showing microvilli (MV) of 500–1000 nm length. Tight junctions (TJ), desmosomes (D), nexus (Nx), mitochondria (M), lysosomes (L) and nuclei (N) are indicated. Scale bar 1,000 nm.

was analyzed by live cell fluorescent imaging, using a confocal laser scanning microscope. Fluorescence images show the cytoplasmic localization of the two fluorescent domains cerulean (Fig. 8A) and mCitrine (Fig. 8B), as well as the occurrence of FRET (Fig. 8C) in resting Caco-2-eCalwy cells. Notably, there is considerable intercellular heterogeneity in biosensor-expression. This was also confirmed by frequency distribution analysis of the mCitrine-concentration in different Caco-2-eCalwy cells. Because fluorescence of the acceptor-domain mCitrine after direct excitation at 514 nm is independent of zinc-binding [19], its fluorescence signal is directly proportional to the sensor-concentration. mCitrine measurements revealed a wide range of sensor-expression within different cells of the same clone (Fig. 8D).

Due to high background fluorescence and light scattering, the sensitivity of confocal microscopy was insufficient for quantification of free zinc in the stably transfected Caco-2-eCalwy clone. As this was not the case with multiphoton laser scanning microscopy, further FRET-measurements were performed using two photon excitation. Fig. 9A compares normalized FRET-emission spectra of Caco-2-eCalwy cells after zinc-depletion by TPEN or addition of excess zinc, showing a twofold decrease in fluorescence of mCitrine in response to saturation with zinc.

Next, sensor-efficiency after stable transfection and performance of the eCalwy sensor after two photon excitation were investigated using two different approaches: FLIM-FRET based on lifetimes of the donor fluorophore, and theoretical photobleaching using fluorescence intensities. FLIM-FRET analysis confirmed proper function of the eCalwy

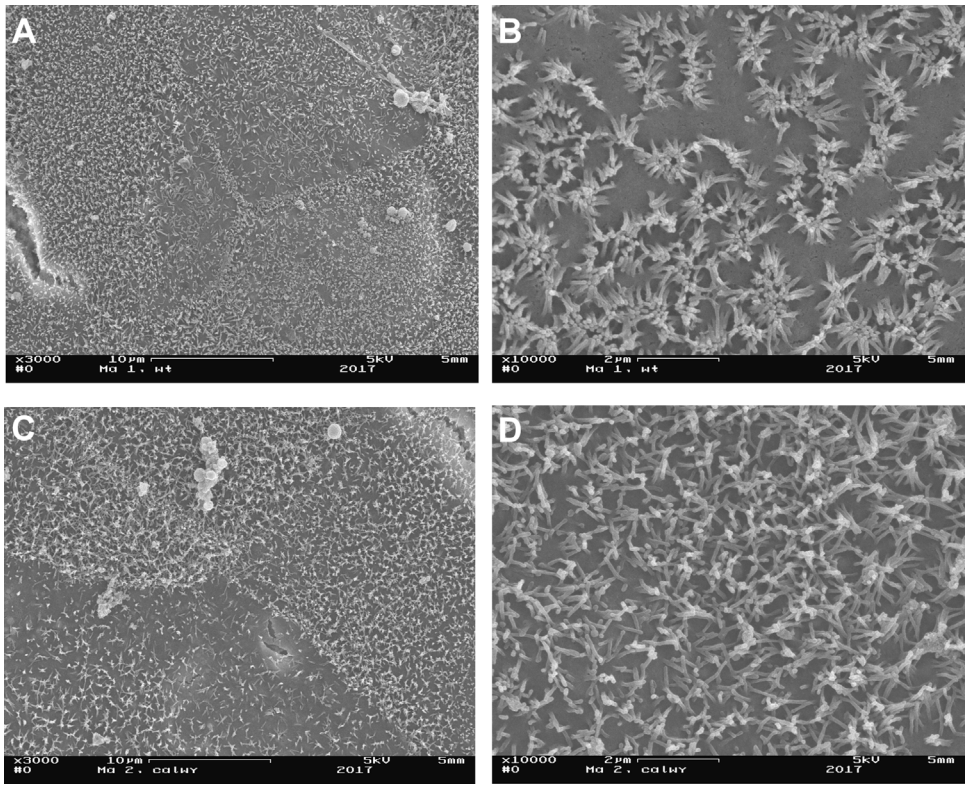

Fig. 3. Scanning electron microscope images. Shown are the apical surface of Caco-2-WT (A, B) and Caco-2-eCALWY clones (C, D). Both cells display characteristic columnar shape (A, C) and microvilli formation (B, D). Scale bars 2 µm (B, D) and 10 µm (A, C).

probe after stable transfection into Caco-2-eCalwy (Fig. 9B). Fluorescence lifetime of the donor-domain (τ_{DA}) cerulean increased significantly after zinc addition (one-way ANOVA, $p < 0.001$). Besides, a significant difference between τ_D (fluorescence lifetime of the donor in the absence of the acceptor-domain mCitrine) and in τ_{DA} was observed. FRET-efficiency is defined as the amount of energy that is transferred from donor to acceptor-domain after excitation [20]. Calculated FRET-efficiencies based on fluorescence lifetime and the actual fluorescence intensities are in good agreement (Fig. 9C), with an energy transfer of about 60% in the resting state (buffer) and 40% after addition of zinc.

Finally, the correlation of sensor-concentration and FRET-ratio was examined with multiphoton microscopy. Despite differences in sensor concentrations of more than one order of magnitude (measured by directly exciting the mCitrine-domain), there was no correlation with the FRET-emission ratio (Fig. 9D). Linear regression analysis of these data provided additional confirmation that the slope is not significantly different from zero. This demonstrates that the expression level of the eCalwy-biosensor had no effect on fractional probe-saturation with zinc.

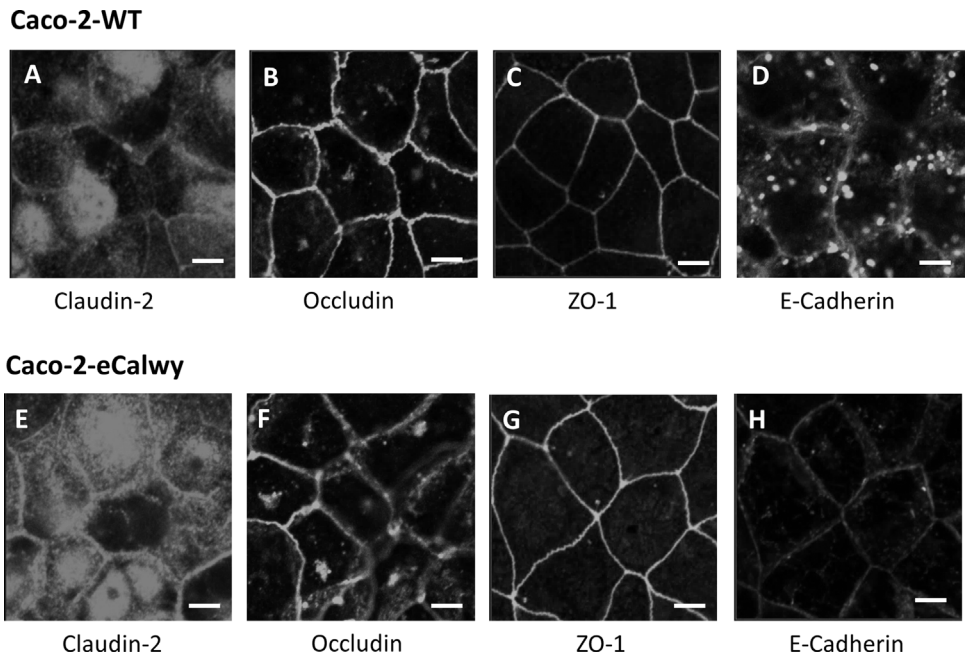

Fig. 4. Localization of tight junction proteins. Fluorescence imaging was conducted using a confocal laser scanning microscope, showing results for differentiated Caco-2-WT (upper panel) and Caco-2-eCALWY (lower panel) cells. Shown are selected images of Caco-2-WT and -eCalwy clones after immunofluorescent staining of claudin-2 (A, E), occludin (B, F), *zonola occludens*-1 (ZO-1) (C, G) and E-cadherin (D, H) of two independent experiments. Scale bar 5 µm.

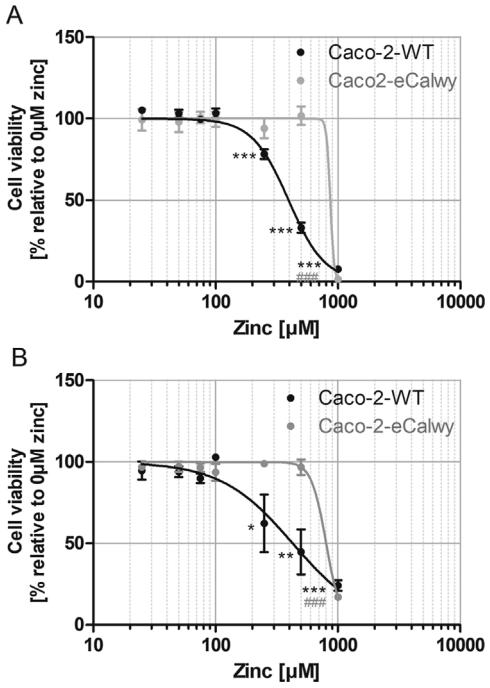

Fig. 5. Zinc-toxicity on differentiated Caco-2-WT and -eCalwy. Cells were treated with different zinc concentrations for 24 h and mitochondrial activity was analyzed using two different assays based on the tetrazolium salts MTT (A) and WST-8 (B). A total of 0.01% Triton X-100 was used as positive control. Data are shown as means ± SD of three independent experiments. Sigmoidal dose–response curves were fitted by nonlinear regression and means significantly different from the untreated controls are indicated (**p < 0.01; ***p < 0.001; one-way ANOVA with Dunnett's multiple comparison test).

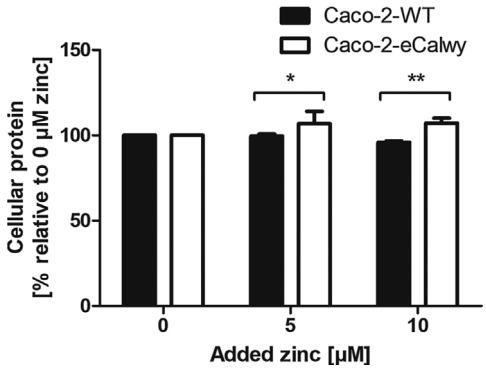

Fig. 6. Effect of zinc on cellular protein levels. Caco-2-WT and -eCALWY cells were cultivated for 21d with different concentrations of zinc added to the culture medium, and protein content was analyzed using the SRB assay. Data are shown as means ± SD of three independent experiments. Significant differences are indicated (*p < 0.05; **p < 0.01; two-way ANOVA with Bonferroni post hoc test).

4. Discussion and conclusion

Several zinc-FRET-biosensors, such as eCalwy, eZinch, and ZapCy2, have been created and were used in various different cell types, but until now only after transient transfection [19,21–24]. This study describes a Caco-2 cell clone stably expressing the zinc-biosensor eCalwy-5. Several approaches were applied to reassure enterocyte specific properties, including morphological characterization as well as investigating the maintenance of the intestinal barrier integrity, especially tight junction formation and epithelial resistance, which need to be considered when using intestinal cell models [25].

ALP-activity is a marker for intestinal cell differentiation and its increasing activity during differentiation of Caco-2 cells was demonstrated before [12]. Moreover, the dependence of intestinal ALP-

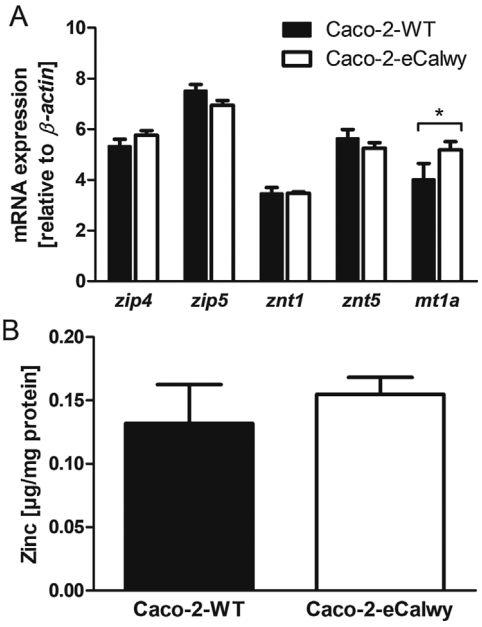

Fig. 7. Zinc homeostasis in Caco-2-WT and -eCalwy. (A) Gene expression of proteins involved in zinc-homeostasis in differentiated Caco-2-WT and Caco-2-eCALWY clones was analyzed by qPCR. (B) Basal zinc content of differentiated Caco-2-WT and Caco-2-eCALWY clones was analyzed using FAAS. Data are shown as means ± SD of three independent experiments. Significant differences between the two cell clones are indicated (*p < 0.05; Student's *t*-test).

activity on zinc availability is well known [26] and might be reflected in Caco-2-eCalwy. Differences in ALP-expression and -activity were observed in the present study, with the ALP-activity of Caco-2-eCalwy being only 50% of that measured in Caco-2-WT. Yet, the activity in Caco-2-eCalwy is still one order of magnitude higher than levels observed in other differentiated intestinal cell lines [27], indicating successful differentiation.

A morphology characteristic for the intestinal brush border membrane was still present after stable transfection of the FRET-biosensor into Caco-2 cells, and is comparable to previous studies with Caco-2-WT cells [27–29]. Comparison of Caco-2-WT and Caco-2-eCalwy clones revealed only slight differences regarding subcellular localization of the tight junction protein occludin, which did not affect basic integrity of the intestinal barrier. Tight junction proteins play a key role in creating a selective transport barrier and maintain cell polarity, while guaranteeing a certain permeability [30]. Claudin-2 is important for paracellular ion permeability and was reported to decrease tightness of the epithelial barrier [31] and to be localized in plasma membrane and cytoplasm of Caco-2-WT cells [32]. The peripheral tight junction protein ZO-1 is crucial for assembly of tight junctions and binds to the transmembrane protein occludin [33]. While both cell clones show typical localization of ZO-1 [33], distribution of occludin in Caco-2-eCalwy differs from Caco-2-WT and observations in previous studies [32,33]. An increase in occludin-expression might elevate TEER and thus could affect the tightness of epithelium [34]. However, no differences in TEER between the two cell clones were observed. The vesicular distribution of E-cadherin in Caco-2-WT clones is no artifact caused by the experimental conditions, because it was not observed in Caco-2-eCalwy cells incubated in parallel. Possibly, excess E-cadherin is internalized in Caco-2-WT cells and E-cadherin-expression in Caco-2-eCalwy is lower as a result of the transfection. Nevertheless, localization and expression of E-cadherin and occludin were shown to be zinc-dependent [33], thus the differences between the two cell clones could also be explained by the introduction of the additional zinc-binding eCalwy-protein. However, E-cadherin is still evenly distributed at the cell-cell junction membrane of both cell clones, where it plays an

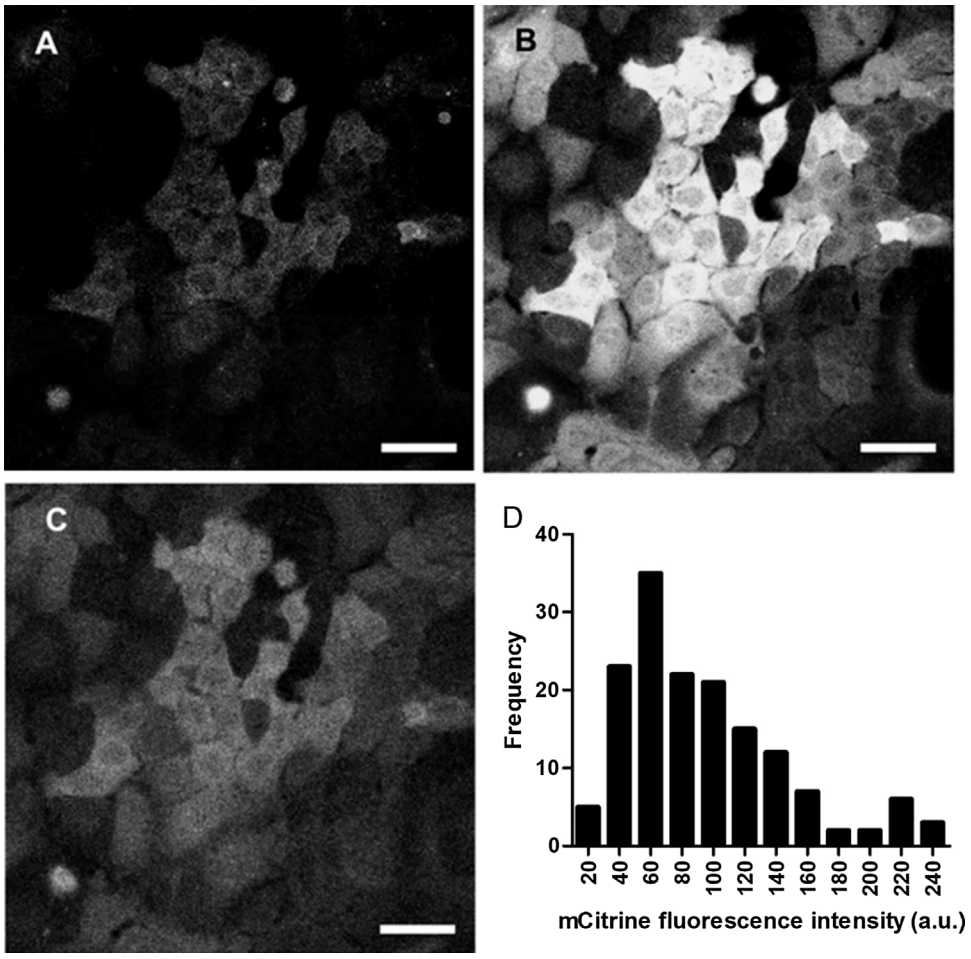

Fig. 8. Life cell imaging. (A–C) Cellular distribution of sensor-protein in Caco-2-eCALWY cells was analyzed by fluorescence live cell imaging using a confocal laser scanning microscope. Shown are fluorescence images of (A) cerulean emission (λ_{ex} = 458 nm; λ_{em} = 462nm–496 nm), (B) mCitrine emission (λ_{ex} = 514 nm; λ_{em} = 526nm–590 nm) and (C) FRET, not corrected for spectral bleed-trough (λ_{ex} = 458 nm; λ_{em} = 526nm–590 nm). Scale bar 50 µm. (D) Frequency distribution of eCALWY-sensor concentration in Caco-2-eCalwy cells, analyzed by direct excitation of mCitrine (λ_{ex} = 458 nm; λ_{em} = 527 nm).

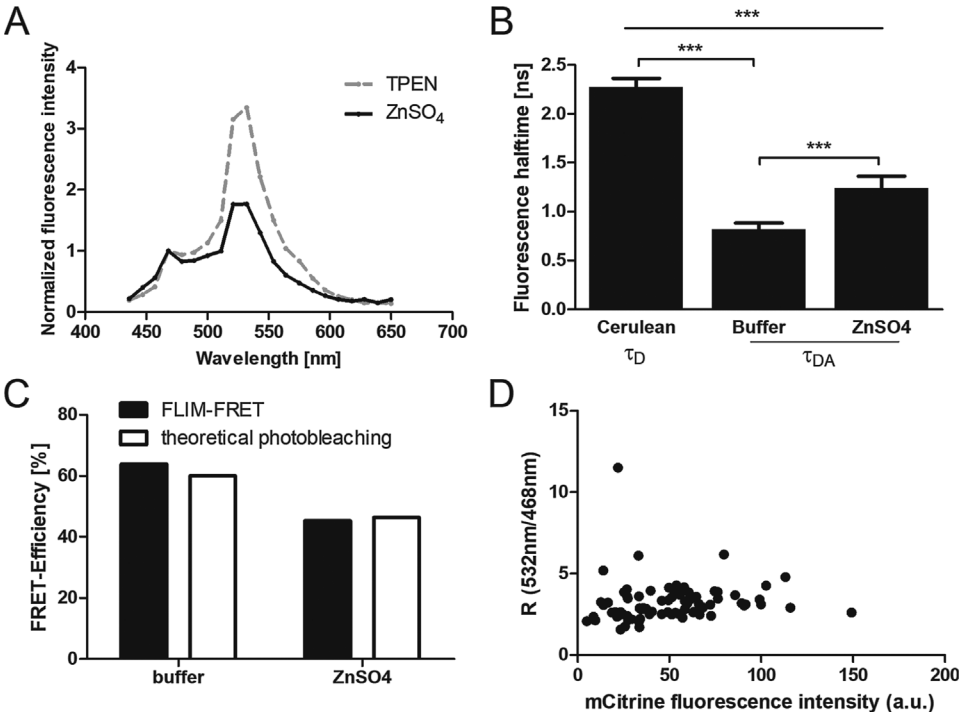

Fig. 9. Two photon microscopy. (A) Emission spectra of Caco-2-eCalwy in the presence of TPEN (20 µM) or zinc (400 µM). (B) Fluorescence lifetime of FRET-donor domain cerulean of eCalwy-biosensor in Caco-2-eCalwy. Fluorescence halftime is shown for the donor in the absence of the acceptor-domain (cerulean), in resting states (buffer) and after addition of zinc. Data are shown as means ± SD of three independent experiments. Significant differences between the fluorophore-lifetimes under the different conditions are indicated (***$p < 0.001$; ANOVA followed by Bonferroni's multiple comparison test). (C) FRET-efficiency of eCalwy-5 in Caco-2-eCalwy cells based on FLIM-FRET-data compared to theoretical calculations using fluorescence intensities. (D) Impact of cellular sensor-expression level on zinc-saturation of the sensor. Shown is the correlation of fluorescence emission ratio (mCitrine/cerulean) and eCALWY-sensor expression, depicted as mCitrine fluorescence when directly excited at 514 nm (λ_{em} = 532 nm) using a multiphoton laser scanning microscope.

important role in cell-cell adhesion during Caco-2 cell differentiation [35]. Taken together, important features of the intestinal cell line Caco-2 were largely preserved during stable transfection.

Intracellular free zinc is regulated by zinc binding proteins, such as MT, maintaining free zinc concentrations in the low or even sub-nanomolar range [36]. Thus, the expression of an additional zinc binding protein, such as eCalwy-5, might interfere with cellular zinc homeostasis, possibly by buffering zinc. Accordingly, investigations of acute zinc toxicity revealed that Caco-2-eCalwy cells were more resistant to high zinc concentrations. We also analyzed the effect of long term administration of sub-toxic concentrations of zinc in addition to the basal content of cell culture medium of 3 µM. Caco-2-WT cells were unaffected, whereas Caco-2-eCalwy seem to require more zinc during differentiation, since the protein level was higher after cultivation in the presence of additional zinc. This indicates that the development of Caco-2-eCalwy cells is already significantly enhanced when cultivated with a 2.7 fold higher zinc concentration. However, the transfection of eCalwy-protein showed only slight effects on intracellular zinc homeostasis, as expression of major intestinal zinc transporters was not impaired, the basal cellular zinc content did not differ, and only *mt1a*-expression was elevated in Caco-2-eCalwy. More precisely, the zinc transporters ZIP4, ZIP5, ZnT-5 and ZnT-1 play a key role in intestinal zinc resorption and together with proteins of the MT-family these transporters are important for maintaining intracellular zinc homeostasis [37]. The slightly elevated *mt1a*-expression in Caco-2-eCalwy clones might therefore also be a reason for the increased resistance against acute zinc toxicity.

Finally, performance of the zinc-biosensor in Caco-2-eCalwy clones and cellular distribution as well as the effect of its expression-level was investigated. Beforehand, sensor-activity had to be scrutinized, since it is well known that the use of multi photon microscopy for sensors created for one photon approaches is not always working properly [38]. FLIM-FRET-measurements confirmed a proper and efficient function of the stably transfected eCalwy-protein. Due to the off-FRET, τ_{DA} increases after zinc-addition, because of the decreased energy transfer to the acceptor-domain. Notably, τ_{DA} in the presence of zinc did not reach the full amount of τ_{D}. This is not surprising, as some remaining energy transfer to the acceptor-domain is always present in the FRET-sensor, even after conformational change due to zinc-binding [9]. In this manner, correct functionality of the eCalwy-sensor after stable transfection into Caco-2 and by two-photon excitation was confirmed as well.

Fluorescence cell imaging showed no organelle-specific distribution of the eCalwy-protein but indicated considerable intercellular heterogeneity in expression of the FRET-biosensor. Quantification of free zinc in the resting state yielded a concentration of ~2 nM, which is in line with previous studies analyzing free zinc with low molecular weight sensors in the intestinal cell line HT29 [39] and other cell lines [40]. It is well known that the introduction of a zinc-binding molecule into cells can perturb cellular zinc homeostasis, which might lead to a disturbance of the cellular equilibria of free and bound zinc [39,41]. Thus the intracellular sensor-concentration must be as low as possible, particularly when analyzing cellular free zinc using synthetic probes, where sensor-concentration was shown to be critical for zinc-quantification [39,42]. However, it remains to be fully understood inasmuch the expression of genetically encoded zinc-sensors impacts zinc-quantification. The expression-level of the eCalwy-biosensor in stably transfected Caco-2-eCalwy cells had no effect on the FRET-ratio. A comparable observation was also reported by Qin et al., where different concentrations of the transiently transfected FRET-biosensor ZapCY2 had no influence on percental saturation of the sensor molecule in Hela cells [24]. Furthermore, in that study, the ZapCY2-sensor was expressed in nucleus and cytoplasm of Hela cells, while Caco-2-eCalwy revealed an even cytoplasmic distribution of the biosensor. In fact, intracellular biosensor-concentrations were estimated to be 1–10 µM [24], which is considerably lower compared to the reported millimolar concentrations of low molecular weight-sensors in cells [41]. Certainly, final low molecular weight sensor-concentration is dependent on its subcellular distribution and volume of the cellular compartment where it accumulates [40], whereas biosensor-concentrations are controlled by their expression and the effect of different expression-levels on their subcellular concentration is yet unknown. Thus, it might be that because both biosensors are localized in the cytoplasm of the cells and not in a smaller organelle, the sensor-concentration was not sufficiently high to influence cellular labile zinc. However, there are several zinc biosensors with organelle-specific targeting [19,21–23]. Therefore it is certainly necessary to further investigate the effect of cellular expression of those organelle-specific biosensors on the quantification of free zinc.

This study describes a well characterized stable Caco-2 cell clone expressing the eCALWY-5 FRET-sensor, which can be used to investigate intestinal zinc resorption. It also highlights the importance of reassuring characteristic features of wildtype cells in the transfected cell clones, as well as the investigation of possible changes in zinc-homeostasis when stably transfecting zinc-biosensors. Furthermore, it is not only crucial to characterize subcellular distribution of the biosensor but also to check the impact of sensor-expression on its zinc-saturation.

Conflict of interest

The authors declare they have no conflict of interest.

Funding

The work of HH is supported by the Deutsche Forschungsgemeinschaft (TraceAge – DFG Research Unit on Interactions of essential trace elements in healthy and diseased elderly, Potsdam-Berlin-Jena, FOR 2558/1, HA 4318/4-1).

Appendix A. Supplementary data

Supplementary data associated with this article can be found, in the online version, at https://doi.org/10.1016/j.jtemb.2018.01.004.

References

[1] M. Maares, H. Haase, Zinc and immunity: an essential interrelation, Arch. Biochem. Biophys. 611 (2016) 58–65.
[2] D. Ford, Intestinal and placental zinc transport pathways, Proc. Nutr. Soc. 63 (1) (2004) 21–29.
[3] R.J. Cousins, J.P. Liuzzi, L.A. Lichten, Mammalian zinc transport, trafficking, and signals, J. Biol. Chem. 281 (34) (2006) 24085–24089.
[4] W. Maret, H.H. Sandstead, Zinc requirements and the risks and benefits of zinc supplementation, J. Trace Elem. Med. Biol. 20 (1) (2006) 3–18.
[5] X. Wang, B. Zhou, Dietary zinc absorption: a play of Zips and ZnTs in the gut, IUBMB Life 62 (3) (2010) 176–182.
[6] G. Cerchiaro, T.M. Manieri, F.R. Bertuchi, Analytical methods for copper, zinc and iron quantification in mammalian cells, Metallomics 5 (10) (2013) 1336–1345.
[7] K.P. Carter, A.M. Young, A.E. Palmer, Fluorescent sensors for measuring metal ions in living systems, Chem. Rev. 114 (8) (2014) 4564–4601.
[8] Z. Huang, S.J. Lippard, Illuminating mobile zinc with fluorescence: from cuvettes to live cells and tissues, Methods Enzymol. 505 (2012) 445–468.
[9] J.L. Vinkenborg, T.J. Nicolson, E.A. Bellomo, M.S. Koay, G.A. Rutter, M. Merkx, Genetically encoded FRET sensors to monitor intracellular Zn2+ homeostasis, Nat. Methods 6 (10) (2009) 737–740.
[10] A.M. Hessels, M. Merkx, Genetically-encoded FRET-based sensors for monitoring Zn (2+) in living cells, Metallomics 7 (2) (2014) 258–266.
[11] M.C. Carpenter, M.N. Lo, A.E. Palmer, Techniques for measuring cellular zinc, Arch. Biochem. Biophys. 611 (2016) 20–29.
[12] S. Ferruzza, C. Rossi, M.L. Scarino, Y. Sambuy, A protocol for in situ enzyme assays to assess the differentiation of human intestinal Caco-2 cells, Toxicol. In Vitro 26 (8) (2012) 1247–1251.
[13] P.K. Smith, R.I. Krohn, G.T. Hermanson, A.K. Mallia, F.H. Gartner, M.D. Provenzano, E.K. Fujimoto, N.M. Goeke, B.J. Olson, D.C. Klenk, Measurement of protein using bicinchoninic acid, Anal. Biochem. 150 (1) (1985) 76–85.
[14] V. Vichai, K. Kirtikara, Sulforhodamine B colorimetric assay for cytotoxicity screening, Nat. Protoc. 1 (3) (2006) 1112–1116.
[15] K.W. Leung, M. Liu, X. Xu, M.J. Seiler, C.J. Barnstable, J. Tombran-Tink, Expression of ZnT and ZIP zinc transporters in the human RPE and their regulation by neurotrophic factors, Invest. Ophthalmol. Vis. Sci. 49 (3) (2008) 1221–1231.
[16] S. Overbeck, P. Uciechowski, M.L. Ackland, D. Ford, L. Rink, Intracellular zinc

homeostasis in leukocyte subsets is regulated by different expression of zinc exporters ZnT-1 to ZnT-9, J. Leukoc. Biol. 83 (2) (2008) 368–380.
[17] K. Wolf, C. Schulz, G.A.J. Riegger, M. Pfeifer, Tumour necrosis factor-α induced CD70 and interleukin-7R mRNA expression in BEAS-2B cells, Eur. Respir. J. 20 (2) (2002) 369–375.
[18] G. Grynkiewicz, M. Poenie, R.Y. Tsien, A new generation of Ca2+ indicators with greatly improved fluorescence properties, J. Biol. Chem. 260 (1985) 3440–3450.
[19] P.J. Dittmer, J.G. Miranda, J.A. Gorski, A.E. Palmer, Genetically encoded sensors to elucidate spatial distribution of cellular zinc, J. Biol. Chem. 284 (24) (2009) 16289–16297.
[20] H. Wallrabe, A. Periasamy, Imaging protein molecules using FRET and FLIM microscopy, Curr. Opin. Chem. Biol. 16 (1) (2005) 19–27.
[21] P. Chabosseau, E. Tuncay, G. Meur, E.A. Bellomo, A. Hessels, S. Hughes, P.R. Johnson, M. Bugliani, P. Marchetti, B. Turan, A.R. Lyon, M. Merkx, G.A. Rutter, Mitochondrial and ER-targeted eCALWY probes reveal high levels of free Zn2+, ACS Chem. Biol. 9 (9) (2014) 2111–2120.
[22] A.M. Hessels, P. Chabosseau, M.H. Bakker, W. Engelen, G.A. Rutter, K.M. Taylor, M. Merkx, EZinCh-2: a versatile, genetically encoded FRET sensor for cytosolic and intraorganelle Zn(2+) imaging, ACS Chem. Biol. 10 (9) (2015) 2126–2134.
[23] Y. Qin, P.J. Dittmer, J.G. Park, K.B. Jansen, A.E. Palmer, Measuring steady-state and dynamic endoplasmic reticulum and Golgi Zn(2+) with genetically encoded sensors, Proc. Natl. Acad. Sci. U. S. A. 108 (18) (2011) 7351–7356.
[24] Y. Qin, J.G. Miranda, C.I. Stoddard, K.M. Dean, D.F. Galati, A.E. Palmer, Direct comparison of a genetically encoded sensor and small molecule indicator: implications for quantification of cytosolic Zn2+, ACS Chem. Biol. 8 (11) (2013) 2366–2371.
[25] E. Le Ferrec, C. Chesne, P. Artusson, D. Brayden, G. Fabre, P. Gires, F. Guillou, M. Rousset, W. Rubas, M.L. Scarino, In vitro models of the intestinal barrier. The report and recommendations of ECVAM Workshop 46. European Centre for the Validation of Alternative methods, Altern. Lab. Anim. 29 (6) (2001) 649–668.
[26] R.B. Williams, Intestinal alkaline phosphatase and inorganic pyrophosphatase activities in the zinc-deficient rat, Br. J. Nutr. 27 (1) (1972) 121–130.
[27] M. Pinto, S. Rabine-Leon, M.-D. Appay, M. Kedinger, N. Triadou, E. Dussaulx, B. Lacroix, P. Simon-Assmann, K. Haffen, J. Fogh, A. Zweigbaum, Enterocyte-like differentiation and polarization of the human colon carcinoma cell line Caco-2 in culture, Biol. Cell 47 (1983) 323–330.
[28] C. Schimpel, O. Werzer, E. Frohlich, G. Leitinger, M. Absenger-Novak, B. Teubl, A. Zimmer, E. Roblegg, Atomic force microscopy as analytical tool to study physicomechanical properties of intestinal cells, Beilstein J. Nanotechnol. 6 (2015) 1457–1466.
[29] J.M. Biazik, K.A. Jahn, Y. Su, Y.-N. Wu, F. Braet, Unlocking the ultrastructure of colorectal cancer cells in vitro using selective staining, World J. Gastroenterol. 16 (22) (2010) 2743–2753.
[30] D. Günzel, A.S.L. Yu, Claudins and the modulation of tight junction permeability, Physiol. Rev. 93 (2) (2013) 525–569.
[31] S. Amasheh, M. Fromm, D. Günzel, Claudins of intestine and nephron – a correlation of molecular tight junction structure and barrier function, Acta Physiol. 201 (1) (2011) 133–140.
[32] A. Fischer, M. Gluth, F. Weege, U.-F. Pape, B. Wiedenmann, D.C. Baumgart, F. Theuring, Glucocorticoids regulate barrier function and claudin expression in intestinal epithelial cells via MKP-1, Am. J. Physiol. Gastrointest. Liver Physiol. 306 (3) (2014) G218–G228.
[33] A. Finamore, M. Massimi, L. Conti Devirgiliis, E. Mengheri, Zinc deficiency induces membrane barrier damage and increases neutrophil transmigration in Caco-2 cells, J. Nutr. 138 (9) (2008) 1664–1670.
[34] K.M. McCarthy, I.B. Skare, M.C. Stankewich, M. Furuse, S. Tsukita, R.A. Rogers, R.D. Lynch, E.E. Schneeberger, Occludin is a functional component of the tight junction, J. Cell Sci. 109 (9) (1996) 2287–2298.
[35] C. Schreider, G. Peignon, S. Thenet, J. Chambaz, M. Pinçon-Raymond, Integrin-mediated functional polarization of Caco-2 cells through E-cadherin—actin complexes, J. Cell Sci. 115 (3) (2002) 543–552.
[36] W. Maret, Molecular aspects of human cellular zinc homeostasis: redox control of zinc potentials and zinc signals, Biometals 22 (1) (2009) 149–157.
[37] M. Murakami, T. Hirano, Intracellular zinc homeostasis and zinc signaling, Cancer Sci. 99 (8) (2008) 1515–1522.
[38] R.N. Day, W. Tao, K.W. Dunn, A simple approach for measuring FRET in fluorescent biosensors using two-photon microscopy, Nat. Protoc. 11 (11) (2016) 2066–2080.
[39] A. Krezel, W. Maret, Zinc-buffering capacity of a eukaryotic cell at physiological pZn, J. Biol. Inorg. Chem. 11 (8) (2006) 1049–1062.
[40] W. Maret, Analyzing free zinc(ii) ion concentrations in cell biology with fluorescent chelating molecules, Metallomics 7 (2) (2015) 202–211.
[41] K.E. Dineley, L.M. Malaiyandi, I.J. Reynolds, A reevaluation of neuronal zinc measurements: artifacts associated with high intracellular dye concentration, Mol. Pharmacol. 62 (3) (2002) 618–627.
[42] H. Haase, S. Hebel, G. Engelhardt, L. Rink, Flow cytometric measurement of labile zinc in peripheral blood mononuclear cells, Anal. Biochem. 352 (2) (2006) 222–230.